Macromolecular Materials and Engineering

Macromolecular Materials and Engineering Open Access

www.mame-journal.de

RESEARCH ARTICLE OPEN ACCESS

Morphology and Structure of PEDOT:Nafion: Insights from Experiment and Molecular Dynamics Simulations

Mohsen Modarresi[1] | Mirko Prato[2] | Stefano Carli[3] | Edoardo Marchini[4] | Igor Zozoulenko[1]

[1]Laboratory of Organic Electronics (LOE), Department of Science and Technology (ITN), Campus Norrköping, Linköping University, Norrköping, Sweden | [2]Materials Characterization Facility, Istituto Italiano di Tecnologia, Genova, Italy | [3]Department of Environmental and Prevention Sciences-DEPS, University of Ferrara, Ferrara, Italy | [4]Department of Chemical Pharmaceutical and Agricultural Sciences, University of Ferrara, Ferrara, Italy

Correspondence: Stefano Carli (crlsfn@unife.it) | Igor Zozoulenko (igor.zozoulenko@liu.se)

Received: 19 December 2025 | **Revised:** 4 February 2026 | **Accepted:** 24 February 2026

Keywords: molecular dynamics | PEDOT:Nafion | XPS | XRD

ABSTRACT

Poly(3,4-ethylenedioxythiophene) (PEDOT)/Nafion is a promising mixed ionic–electronic conducting polymer. However, in contrast to the well-studied PEDOT:poly(styrenesulfonate) (PSS) system, the nanoscale morphology and the relationship between crystallinity and composition in PEDOT/Nafion remain insufficiently explored and therefore poorly understood. In this work, we investigate the morphology and structural organization of PEDOT/Nafion by combining X-ray photoelectron spectroscopy (XPS), X-ray diffraction (XRD), and coarse-grained molecular dynamics (MD) simulations. This combined approach enables us to directly link surface composition, bulk crystallinity, and molecular-scale packing in PEDOT/Nafion—insights that are not accessible from PEDOT:PSS or Nafion-only studies. XPS revealed two distinct sulfur environments associated with PEDOT and Nafion, with a sulfonic-acid-to-thiophene-group ratio $R_{S/T}$ of ≈ 2.3. XRD analysis showed PEDOT crystallites with an average π–π stacking size of about 2.1 nm. MD simulations provided molecular-level insight into the effect of composition, demonstrating that higher Nafion content disrupts PEDOT stacking, yielding smaller crystallites (~1.1 nm), while reduced Nafion content promotes better ordering (~1.4–1.8 nm). These findings establish a clear correlation between composition and crystallinity, supporting a model where the surface is Nafion-rich and the bulk has a lower $R_{S/T}$ ratio. The combined experimental–computational approach offers a comprehensive understanding of PEDOT morphology and valuable guidance for the design of mixed ion–electron conducting polymers.

1 | Introduction

Mixed ionic–electronic conducting polymers, which support simultaneous ionic and electronic transport, have attracted growing interest in materials science due to their unique combination of electrical, mechanical, and thermal properties, enabling applications in devices that rely on coupled ion–electron conduction such as supercapacitors, sensors, ion pumps, electrochemical transistors, and many others [1–4]. Among these polymers, poly(3,4-ethylenedioxythiophene):polystyrenesulfonate (PEDOT:PSS) is probably the most useful, versatile, and studied [5–7]. In fact, PEDOT:PSS exhibits a large set of appealing properties, such as high conductivity, large capacitance values, high dispersibility in water, which facilitate the deposition of this conductive polymer on different substrates. In addition, PEDOT:PSS is also highly chemically and electrochemically stable. One of the most important properties of PEDOT:PSS films is their extremely high conductivity that after post-treatment can reach values as high as 1000–3000 S/cm, thereby resulting almost comparable to metallic conductor surfaces [8, 9].

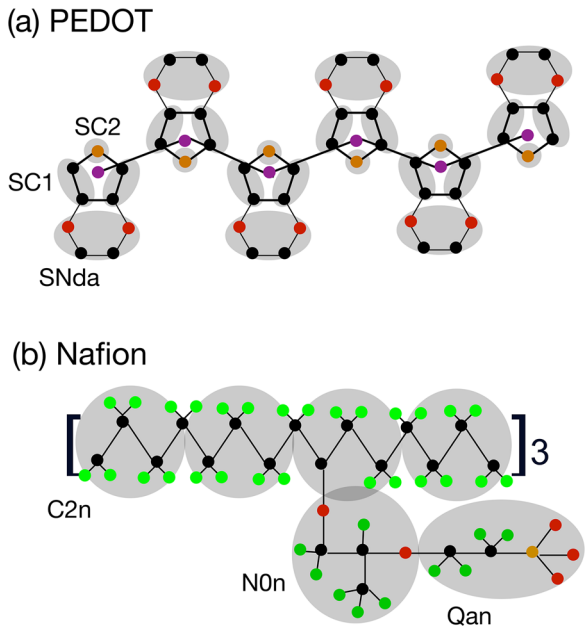

FIGURE 1 | (a) The atomic structure and the Martini coarse-grained beads for (a) PEDOT and (b) Nafion. Colour scheme: black (C), red (O), yellow (S), green (F), purple (virtual sites). The Martini beads are SC1, SC2, and SNda for PEDOT and C2n, Non, Qan for nafion.

Recently, the novel conducting polymer PEDOT:Nafion was synthesized via a reproducible protocol from water-based dispersion of the monomer EDOT in the presence of the ionomer Nafion [10], see Figure 1 for a chemical structure of PEDOT and Nafion. The PEDOT:Nafion film exhibits a conductivity range of 0.3–2 S/cm, which can be enhanced up to approximately 6 S/cm by ethylene glycol treatment. Interestingly, PEDOT:Nafion demonstrates improved adhesion to glass substrates compared to PEDOT:PSS without silane cross-linkers [10]. The PEDOT:Nafion coating on flexible neural microelectrodes provides similar in vivo recording quality as PEDOT:PSS, while allowing a much higher charge injection due to the reduced polarization during electrical stimulation [11]. Melt-spun PEDOT:Nafion fibers can be fabricated showing excellent mechanical properties with the nontoxicity of the material [12]. This makes PEDOT:Nafion a good candidate for organic electronic device architectures such as organic electrochemical transistors, artificial synapses [12], and chronic bioelectronic applications.

Despite the growing interest in PEDOT:Nafion and its promising performance in mixed ionic–electronic conducting applications, its detailed morphology and structural organization remain poorly understood. By contrast, the morphology of PEDOT:PSS system is relatively well established: PEDOT:PSS can be described as a three-component system comprising positively charged PEDOT chains, deprotonated negatively charged PSS chains, and protonated neutral PSS chains [13, 14]. In this framework, PEDOT-rich domains are dominated by PEDOT and deprotonated PSS, whereas PSS-rich domains consist largely of protonated PSS. In contrast to the extensively studied PEDOT:PSS systems, or Nafion systems [15, 16], only limited information is available regarding the molecular arrangement, phase separation, and crystallinity of PEDOT:Nafion films. Understanding these structural features is essential, as they directly influence charge transport, ion mobility, and interfacial properties that determine device performance.

To date, no systematic computational studies have been reported that provide molecular-level insight into the morphology of PEDOT:Nafion. In particular, simulations developed for PEDOT:PSS do not account for Nafion's fluorinated backbone, and Nafion-only simulations cannot describe how PEDOT packing and crystallite formation are modified by the ionomer environment. Notably, *computational microscopy* based on molecular dynamics (MD) simulations represents a powerful yet underutilized approach for elucidating the nanoscale organization of mixed ion–electron conducting polymers [17]. Such simulations can yield reliable and detailed information about key aspects of morphology—such as chain packing, crystallite formation, and polymer–polymer interactions—that are difficult to access experimentally.

In this work, we investigate the morphology and structure of PEDOT:Nafion films by combining X-ray photoelectron spectroscopy (XPS) and X-ray diffraction (XRD) measurements with coarse-grained MD simulations. XPS was employed to probe the surface composition and determine the sulfonic-acid-to-thiophene-group ratio $R_{S/T}$, while XRD provided information about the crystalline domain size in the bulk. The experimental observations were then analyzed and interpreted using computational microscopy, enabling us to connect the molecular-scale structure with the measured macroscopic properties.

Our results reveal that the PEDOT:Nafion films exhibit compositional gradients between the surface and the bulk, with the surface enriched in Nafion and the bulk dominated by PEDOT:Nafion with a lower $R_{S/T}$ ratio (i.e. lower Nafion content). Together, these experimental and computational insights provide a coherent picture of PEDOT:Nafion morphology and establish a framework for rational design of mixed-conducting polymer systems for bioelectronic and electrochemical applications.

2 | Model and Methods

2.1 | Experimental Method

2.1.1 | Synthesis of PEDOT:Nafion Film

PEDOT:Nafion was prepared through oxidative polymerization of EDOT in a water dispersion of $FeCl_3$ and Nafion, according to a previously published protocol [10]. Briefly, 3,4-ethylenedioxythiophene (EDOT, 0.187 mmol) was dissolved under N_2 in a dispersion of Nafion (2 mL) in water (6 mL) through vigorous stirring. $FeCl_3$ (0.374 mmol) was added to the mixture, and the stirring was continued at room temperature for 24 h, under N_2 atmosphere. The crude product centrifuged several times with water to give a dark blue dispersion of PEDOT:Nafion in water [10]. Coatings of PEDOT:Nafion were obtained by drop casting the water dispersion on glass slides and the solvent was evaporated at room temperature for 24 h. Deposited films were subjected to an annealing at 100°C for 30 min to improve the adhesion with the glass substrate. This annealing protocol was selected based on the previously reported preparation procedure and to ensure reproducible film formation;

systematic optimization of annealing parameters was outside the scope of the present study.

2.1.2 | Characterization of the PEDOT:Nafion Film

2.1.2.1 | X-ray Photoelectron Spectroscopy (XPS). The surface chemistry of the PEDOT:Nafion films was investigated via XPS. The spectra were collected with a Kratos Axis Ultra^{DLD} spectrometer, using an Al Kα source operated at 20 mA and 15 kV. Survey scans were carried out at a pass energy of 160 eV, over an analysis area of 300 × 700 microns. High-resolution scans were carried out at a pass energy of 20 eV, over the same analysis area, with a specific focus on the S 2p signals. Spectra were analyzed using CasaXPS software (version 2.3.24). Due to spin-orbit coupling, S 2p states were fitted with doublets of peaks having the same full width at half maximum, a spin-orbit splitting (i.e., the distance between the two components of each doublet) of 1.2 eV, and an intensity ratio of 1:2 between the high- and the low-binding energy component ($2p_{1/2}$ and $2p_{3/2}$, respectively). The position of each S 2p doublet is identified by the position of the $2p_{3/2}$ component. The XPS analysis was performed over three different regions of PEDOT:Nafion coating to provide the relative content of thiophene and sulfonate groups as measured on the different areas of the film, as summarized in Table S1.

2.1.2.2 | X-ray diffraction (XRD). XRD pattern was recorded on a Malvern-PANalytical Empyrean X-ray diffractometer equipped with a 1.8 kW CuKα ceramic X-ray tube, PIXcel3D 2 × 2 area detector and operating at 45 kV and 40 mA. The analysis was carried out in the air, at room temperature, using Parallel-Beam (PB) geometry and symmetric reflection mode.

2.2 | Molecular Dynamics Simulations of PEDOT:Nafion Film

For molecular dynamics simulations, we use our previously developed Martini coarse-grained model for PEDOT [17, 18], see Figure 1a. This model has been used to investigate PEDOT solutions, and dried film with different counter ions (Tos, and PSS) and ion diffusion in these systems [9, 13, 14, 17, 18]. The Martini model [19, 20] uses a coarse-grained representation of the polymer, where a single bead represents a few real atoms. The interactions between the beads are described by a simplified force field that is validated by comparison with all-atom simulations, which show that the model reproduces key structural features relevant for morphology, including chain packing and π–π stacking tendencies. For Nafion, we adopted the previous model used to study Nafion aggregation in water [21]. In our simulations, we used the GROningen MAChine for Chemical Simuation (GROMACS) software package to perform molecular dynamics simulations of PEDOT:Nafion in water [22, 23].

In the calculations, the chain length of PEDOT was set to 12 monomer units [24], and the Nafion chain length was set to three monomer units [21]. Note that detailed experimental information on the PEDOT chain length is lacking due to the challenges associated with its experimental determination, primarily arising from the insolubility of PEDOT films. Nevertheless, PEDOT chains are generally believed to be relatively short (N ≈ 10–20). The chain length chosen in the present work (N = 12) is based on our previous molecular dynamics simulations of PEDOT polymerization [24]. The oxidation level of PEDOT was set to 33% (i.e. one positive charge over three monomers), which was compensated by the equal amount of negative charges on Nafion. This choice corresponds to typical experimental conditions for pristine (as-polymerized) PEDOT [25]. We first randomly distributed PEDOT and Nafion chains in the simulation box, which is then filled with polarizable water molecules. The simulation box had the size $25 \times 25 \times 25$ nm^3, and it contained 300 PEDOT chains, 400 Nafion chains, and 86 500 water molecules. The simulation box was equilibrated using a series of energy minimization and equilibration steps. The energy minimization was done by the steepest descent method, followed by equilibration in the Isothermal–isobaric (NPT) ensemble for 50 ns, utilizing the Berendsen barostat and Berendsen thermostat [26]. In the equilibration, a restraint was applied to the polymer matrix to reach an equilibrated water distribution around the PEDOT and Nafion chains. We then performed production runs of 250 ns each, during which we monitored PEDOT's structural and dynamic properties by using the Parrinello-Rahman barostat [27] at $P = 1$ bar and v-rescale thermostat [28] at T = 300 K. In all calculations the Coulomb interaction was calculated using the Particle Mesh Ewald (PME) method [29]. The cut-off distance for the Lennard-Jones interaction was set to 1.4 nm.

The final PEDOT:Nafion solution is dried in 57 successive steps by randomly removing remaining water molecules from the simulation box. This stepwise computational evaporation protocol is a representation of a gradual solvent removal during experimental drop-casting, allowing morphological reorganization between evaporation steps. Here we follow a similar protocol that we used in our previous MD studies of PEDOT:PSS to ensure that the computational solvent removal is sufficiently slow and does not lead to structural or morphological artifacts [13, 14]. The remaining water molecules are equilibrated for 4 ns with a protocol similar to the above. The production run in the NPT ensemble is performed for 8 ns for each evaporation step. As a result, the total molecular dynamics simulation from the initial PEDOT:Nafion solution to the dried film is nearly 1 μs.

3 | Results and Discussion

The S 2p spectrum from XPS analysis reported in Figure 2 displays the typical signals at approximately 164 and 169 eV, which are due to sulfur atoms in the thiophene moiety of EDOT and in the sulfonic acid group of Nafion, respectively [30]. The ratio between the areas of the two signals can be used to infer the thiophene to sulfonic acid groups ratio ($R_{S/T}$) in Pedot:Nafion. According to our XPS analysis, an $R_{S/T}$ value of 2.4 ± 0.3 was found, in line with previous data for PEDOT:Nafion deposited on the same material.

From the XRD pattern shown in Figure 3a a rough estimation of the PEDOT average crystallite size in the π–π stacking direction can be obtained by applying the Scherrer equation on the full width at half maximum (FWHM) of the peak at around $2\theta = 17°$. The value thus obtained is 2.1 nm. We note that the Scherrer equation provides an approximate estimate of coherent scattering length and can be affected by other peak broadening

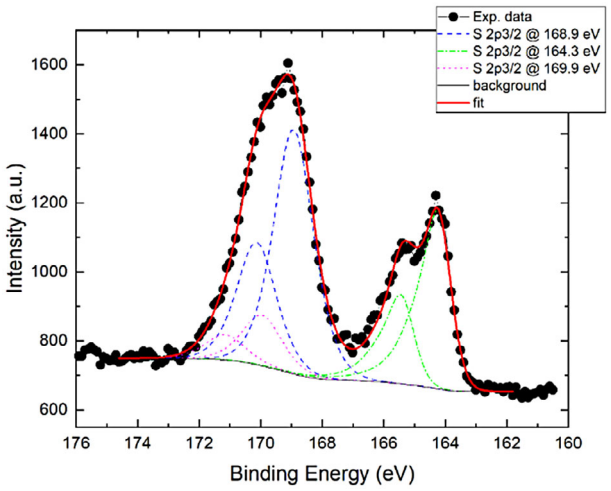

FIGURE 2 | XPS analysis of PEDOT:Nafion film.

contributions (e.g., disorder/strain) commonly present in semi-crystalline polymer systems; thus, the value should be regarded as an effective crystallite-size estimate.

To gain deeper insight into the experimental findings, we employed a *computational microscopy* approach based on coarse-grained molecular dynamics (MD) simulations to model and analyse the morphology of PEDOT:Nafion blends. A representative snapshot of the simulated film morphology is shown in Figure 3c, revealing the formation of PEDOT crystallites surrounded by entangled Nafion chains. (Details of the MD simulations and PEDOT:Nafion film preparation are provided in the Method section).

The degree of stacking between PEDOT chains was quantified through the radial distribution function (RDF) calculated between PEDOT planes in the dried films for various Nafion-to-PEDOT ratios, as shown in Figure 3b. While the X-ray diffraction (XRD) pattern can, in principle, be derived directly from the simulated morphology, the RDF provides a more direct and detailed picture of local ordering. In particular, the number of peaks in the RDF corresponds to the number of stacked chains plus one, allowing the direct estimation of the crystalline domain size.

At a high Nafion content ($R_{S/T} = 2.3$), three peaks are visible in the RDF at normalized distances $R/R_{\pi\pi} = 1, 2, 3$, where $R_{\pi\pi} \approx 3.5$ Å represents the π–π stacking distance. This indicates stacking of four PEDOT chains, corresponding to an average crystallite size of approximately 3×3.5 Å ≈ 1.1nm —roughly half the value (2.1 nm) estimated from the experimental XRD analysis (Figure 2a). As discussed below, this discrepancy is consistent with a Nafion-enriched surface probed by XPS vs. a lower Nafion content in the bulk dominating the XRD signal. When the Nafion content is reduced ($R_{S/T} = 1.15$ and 0.57), additional peaks emerge in the RDF at $R/R_{\pi\pi} = 4$ and 5, corresponding to stacks of five and six chains, respectively. The associated crystallite sizes (≈ 1.4–1.8 nm) are in much better agreement with the experimental value.

It is important to note that XPS probes only the surface region of the film—typically a few nanometers deep. In contrast, the XRD signal integrates over the film thickness and is therefore dominated by the bulk region. Our interpretation thus assumes a compositional gradient across the film thickness, with a Nafion-enriched surface and a bulk region of lower Nafion content. Therefore, the experimentally observed $R_{S/T}$ ratio of ≈ 2.3 primarily reflects the surface composition. Previous studies have reported that the outermost layers of PEDOT:Nafion are enriched in fluorine due to the segregation of sulfonic acid groups away from the surface [10]. Our combined MD and XRD analysis support this interpretation, suggesting that the experimentally observed XRD pattern predominantly originates from the bulk region, where the effective Nafion/PEDOT (or $R_{S/T}$) ratio is lower (< 1) than that at the surface ($R_{S/T} \approx 2.3$).

4 | Conclusion

In this work, we investigated the morphology and structural organization of PEDOT:Nafion films by combining experimental techniques—X-ray photoelectron spectroscopy (XPS) and X-ray diffraction (XRD)—with coarse-grained molecular dynamics (MD) simulations. The XPS spectra revealed two distinct sulfur environments corresponding to the thiophene units of PEDOT and the sulfonic acid groups of Nafion, with an $R_{S/T}$ ratio of approximately 2.3. XRD analysis yielded an average PEDOT crystallite size of about 2.1 nm along the π–π stacking direction.

Complementary MD simulations provided molecular-level insight into the crystallization behavior and its dependence on composition. The simulations revealed that increasing the Nafion content disrupts PEDOT stacking, leading to smaller crystalline domains. Specifically, at a high $R_{S/T}$ ratio of 2.3, the simulated crystallite size (≈1.1 nm) was about half of the experimental value, whereas lowering the Nafion content (ratios 1.15 and 0.57) led to the formation of larger crystalline domains (≈1.4–1.8 nm), in better agreement with the XRD results. Taken together, these findings indicate a strong correlation between local composition and structural ordering in PEDOT:Nafion films. From an application perspective, Nafion content is also expected to influence operational stability through its impact on water uptake, ionic-domain connectivity, mechanical integrity, and interfacial adhesion. While a systematic stability study vs. composition is beyond the scope of the present work, prior reports on PEDOT:Nafion indicate promising performance in bioelectronic contexts and good adhesion/processing robustness [10–12]. Future work will quantify stability metrics (e.g., conductivity retention, electrochemical cycling stability, and mechanical durability) as a function of Nafion content.

The simulations support a model in which the surface region is enriched in Nafion, while the bulk exhibits lower Nafion content and higher PEDOT crystallinity. This compositional gradient explains the observed differences between surface-sensitive (XPS) and bulk-sensitive (XRD) measurements and calculations. The combined experimental–computational approach thus provides a comprehensive understanding of the hierarchical structure of PEDOT:Nafion, offering valuable insight for the design and optimization of mixed-conducting polymer systems in electrochemical and electronic applications. More broadly, this workflow—linking surface-sensitive composition probes and bulk crystallinity measurements with computational

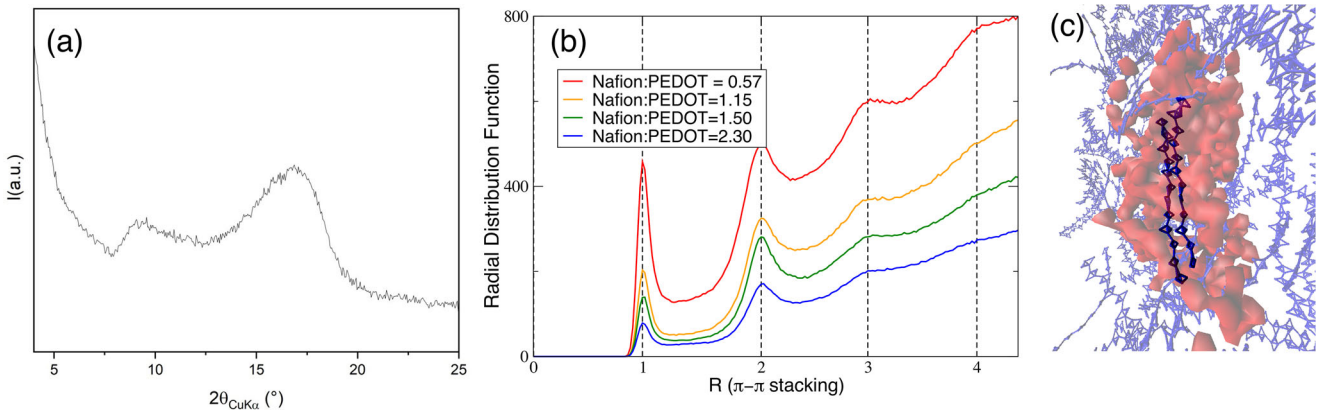

FIGURE 3 | (a) The experimental XRD-pattern of PEDOT:Nafion. (b) The radial distribution function between PEDOT planes at different Nafion:PEDOT ratio indicated in the inset. (c) Snapshots of PEDOT crystallite (blue color) and surrounded Nafion (red color) from MD simulation.

microscopy—can be extended to other mixed ionic–electronic conductors and ionomer–conjugated polymer composites where nanoscale segregation and surface–bulk gradients govern function.

Acknowledgements

I.Z. acknowledges support from Swedish Government Strategic Research Area in Materials Science on Advanced Functional Materials at Linköping University (Faculty Grant SFO-Mat-LiU No. 2009–00971), Swedish Research Council (2024–04449), and Knut and Alice Wallenberg Foundation (KAW) through the Wallenberg Wood Science Center 3.0 (KAW 2021.0313). The computations were performed on resources provided by the National Academic Infrastructure for Supercomputing in Sweden (NAISS).

Conflicts of Interest

The authors declare no conflicts of interest.

Data Availability Statement

The data that support the findings of this study are available from the corresponding authors upon reasonable request.

References

1. M. Berggren, X. Crispin, S. Fabiano, et al., "Ion Electron–Coupled Functionality in Materials and Devices Based on Conjugated Polymers," *Advanced Materials* 31 (2019): 1805813, https://doi.org/10.1002/adma.201805813.

2. B. D. Paulsen, K. Tybrandt, E. Stavrinidou, and J. Rivnay, "Organic Mixed Ionic–Electronic Conductors," *Nature Materials* 19 (2020): 13–26, https://doi.org/10.1038/s41563-019-0435-z.

3. R. Wu, M. Matta, B. D. Paulsen, and J. Rivnay, "Operando Characterization of Organic Mixed Ionic/Electronic Conducting Materials," *Chemical Reviews* 122 (2022): 4493–4551, https://doi.org/10.1021/acs.chemrev.1c00597.

4. S. T. Keene, V. Gueskine, M. Berggren, G. G. Malliaras, K. Tybrandt, and I. Zozoulenko, "Exploiting Mixed Conducting Polymers in Organic and Bioelectronic Devices," *Physical Chemistry Chemical Physics* 24 (2022): 19144–19163, https://doi.org/10.1039/D2CP02595G.

5. A. Elschner, S. Kirchmeyer, W. Lovenich, U. Merker, and K. Reuter, *PEDOT: Principles and Applications of an Intrinsically Conductive Polymer*. (CRC Press, 2010), https://doi.org/10.1201/b10318.

6. D. C. Martin, J. Wu, C. M. Shaw, et al., "The Morphology of Poly(3,4-Ethylenedioxythiophene)," *Polymer Reviews* 50 (2010) 340–384, https://doi.org/10.1080/15583724.2010.495440.

7. I. Zozoulenko, J. F. Franco-Gonzalez, V. Gueskine, et al., "Electronic, Optical, Morphological, Transport, and Electrochemical Properties of PEDOT: a Theoretical Perspective," *Macromolecules* 54 (2021): 5915–5934, https://doi.org/10.1021/acs.macromol.1c00444.

8. H. Shi, C. Liu, Q. Jiang, and J. Xu, "Effective Approaches to Improve the Electrical Conductivity of PEDOT:PSS: a Review," *Advanced Electronic Materials* 1 (2015): 1500017, https://doi.org/10.1002/aelm.201500017.

9. M. Modarresi and I. Zozoulenko, "Why does solvent treatment increase the conductivity of PEDOT : PSS? Insight From molecular dynamics simulations," *Physical Chemistry Chemical Physics* 24 (2022): 22073–22082, https://doi.org/10.1039/D2CP02655D.

10. S. Carli, M. Di Lauro, M. Bianchi, et al., "Water-Based PEDOT:Nafion Dispersion for Organic Bioelectronics," *ACS Applied Materials & Interfaces* 12 (2020): 29807–29817, https://doi.org/10.1021/acsami.0c06538.

11. S. Carli, M. Bianchi, E. Zucchini, et al., "Electrodeposited PEDOT:Nafion Composite for Neural Recording and Stimulation," *Advanced Healthcare Materials* 8 (2019): 1900765, https://doi.org/10.1002/adhm.201900765.

12. A. I. Hofmann, I. Östergren, Y. Kim, et al., "All-Polymer Conducting Fibers and 3D Prints via Melt Processing and Templated Polymerization," *ACS Applied Materials & Interfaces* 12 (2020): 8713–8721, https://doi.org/10.1021/acsami.9b20615.

13. M. Modarresi, A. Mehandzhiyski, M. Fahlman, K. Tybrandt, and I. Zozoulenko, "Microscopic Understanding of the Granular Structure and the Swelling of PEDOT:PSS," *Macromolecules* 53 (2020): 6267–6278, https://doi.org/10.1021/acs.macromol.0c00877.

14. T. Sedghamiz, A. Y. Mehandzhiyski, M. Modarresi, M. Linares, and I. Zozoulenko, "What Can We Learn About PEDOT:PSS Morphology From Molecular Dynamics Simulations of Ionic Diffusion?," *Chemistry of Materials* 35 (2023): 5512–5523, https://doi.org/10.1021/acs.chemmater.3c00873.

15. S. Cui, J. Liu, M. E. Selvan, D. J. Keffer, B. J. Edwards, and W. V. Steele, "A Molecular Dynamics Study of a Nafion Polyelectrolyte Membrane and the Aqueous Phase Structure for Proton Transport," *The Journal of Physical Chemistry B* 111 (2007): 2208–2218, https://doi.org/10.1021/jp066388n.

16. A. Kusoglu and A. Z. Weber, "New Insights Into Perfluorinated Sulfonic-Acid Ionomers," *Chemical Reviews* 117 (2017): 987–1104, https://doi.org/10.1021/acs.chemrev.6b00159.

17. M. Modarresi, J. F. Franco-Gonzalez, and I. Zozoulenko, "Computational Microscopy Study of the Granular Structure and pH Dependence

of PEDOT:PSS," *Physical Chemistry Chemical Physics* 21 (2019): 6699–6711, https://doi.org/10.1039/C8CP07141A.

18. M. Modarresi, J. F. Franco-Gonzalez, and I. Zozoulenko, "Morphology and Ion Diffusion in PEDOT:Tos. A Coarse Grained Molecular Dynamics Simulation," *Physical Chemistry Chemical Physics* 20 (2018): 17188–17198, https://doi.org/10.1039/C8CP02902D.

19. R. Alessandri, F. Grünewald, and S. J. Marrink, "The Martini Model in Materials Science," *Advanced Materials* 33 (2021): 2008635, https://doi.org/10.1002/adma.202008635.

20. S. J. Marrink, L. Monticelli, M. N. Melo, R. Alessandri, D. P. Tieleman, and P. C. T. Souza, "Two Decades of Martini: Better Beads, Broader Scope," *WIREs Computational Molecular Science* 13 (2023): 1620, https://doi.org/10.1002/wcms.1620.

21. T. Mabuchi, S. Huang, and T. Tokumasu, "Nafion Ionomer Dispersion in Mixtures of 1-Propanol and Water Based on the Martini Coarse-Grained Model," *Journal of Polymer Science* 58 (2020): 487–499, https://doi.org/10.1002/pol.20190101.

22. S. Páll, M. J. Abraham, C. Kutzner, B. Hess, and E. Lindahl, "Tackling Exascale Software Challenges in Molecular Dynamics Simulations With GROMACS", (S. Markidis, E. Laure Eds.) *Solving Software Challenges for Exascale* (Springer International Publishing, 2015), pp. 3–27, https://doi.org/10.1007/978-3-319-15976-8_1.

23. M. J. Abraham, T. Murtola, R. Schulz, et al., "GROMACS: High Performance Molecular Simulations Through Multi-level Parallelism From Laptops to Supercomputers," *SoftwareX* 1–2 (2015): 19–25, https://doi.org/10.1016/j.softx.2015.06.001.

24. D. Kim, J. F. Franco-Gonzalez, and I. Zozoulenko, "How Long Are Polymer Chains in Poly(3,4-ethylenedioxythiophene):Tosylate Films? An Insight From Molecular Dynamics Simulations," *The Journal of Physical Chemistry B* 125 (2021): 10324–10334, https://doi.org/10.1021/acs.jpcb.1c04079.

25. D. Kim and I. Zozoulenko, "Why Is Pristine PEDOT Oxidized to 33%? A Density Functional Theory Study of Oxidative Polymerization Mechanism," *The Journal of Physical Chemistry B* 123 (2019): 5160–5167, https://doi.org/10.1021/acs.jpcb.9b01745.

26. H. J. C. Berendsen, J. P. M. Postma, W. F. van Gunsteren, A. DiNola, and J. R. Haak, "Molecular Dynamics With Coupling to an External Bath," *The Journal of Chemical Physics* 81 (1984): 3684–3690, https://doi.org/10.1063/1.448118.

27. M. Parrinello and A. Rahman, "Polymorphic Transitions in Single Crystals: a New Molecular Dynamics Method," *Journal of Applied Physics* 52 (1981): 7182–7190, https://doi.org/10.1063/1.328693.

28. G. Bussi, D. Donadio, and M. Parrinello, "Canonical Sampling Through Velocity Rescaling," *The Journal of Chemical Physics* 126 (2007): 014101, https://doi.org/10.1063/1.2408420.

29. U. Essmann, L. Perera, M. L. Berkowitz, T. Darden, H. Lee, and L. G. Pedersen, "A Smooth Particle Mesh Ewald Method," *The Journal of Chemical Physics* 103 (1995): 8577–8593, https://doi.org/10.1063/1.470117.

30. G. Zotti, S. Zecchin, G. Schiavon, et al., "Electrochemical and XPS Studies Toward the Role of Monomeric and Polymeric Sulfonate Counterions in the Synthesis, Composition, and Properties of Poly(3,4-ethylenedioxythiophene)," *Macromolecules* 36 (2003): 3337–3344, https://doi.org/10.1021/ma021715k.

Supporting Information

Additional supporting information can be found online in the Supporting Information section.

Supporting File: mame70204-sup-0001-SuppMat.docx.